

Atomic models, domain-wall arrangement, and electronic structure of the dense Pb/Si(111)- $\sqrt{3}\times\sqrt{3}$ phase

M. Hupalo, T. L. Chan, C. Z. Wang, K. M. Ho, and M. C. Tringides

Department of Physics, Iowa State University, Ames, Iowa 50011

(Received 3 June 2002; published 31 October 2002)

Despite extensive work in the literature, the structure of the dense Si(111)-Pb($\sqrt{3}\times\sqrt{3}$) phase (ideal coverage $\theta=4/3$ ML) is still unknown because a variety of phases can form, within few percent coverage variation. These phases differ in the way equivalent $\sqrt{3}\times\sqrt{3}$ domains self-organize in different patterns with different domain-wall arrangements. With scanning tunneling microscopy and first-principles calculations we have identified the atomic structure within domains, domain-wall arrangement, and the binding site (H3 or T4) occupied by Pb atoms within each domain.

DOI: 10.1103/PhysRevB.66.161410

PACS number(s): 68.55.Jk, 61.14.Hg, 68.37.Ef

Extensive work with several complementary techniques to identify the structure of the different low-coverage phases on Pb/Si(111) has been carried out over the last 20 years with scanning tunneling microscopy (STM) and diffraction.¹⁻⁹ Part of the motivation is to understand the formation of a variety of phases, which results in a highly complex and poorly understood phase diagram. The origin of the phases is the elastic substrate-mediated interactions because of the large lattice mismatch (9%) between the Pb(111) and Si(111) lattices. Such strain related interactions are long range and have been responsible for pattern formation in other systems i.e., the herringbone Au(111)- $\sqrt{3}\times\sqrt{3}$ reconstruction¹⁰ and preferred domain selection on the reconstructed Si(100)-(2 \times 1) (Ref. 11).

Fundamental questions about the nature of the phases still remain open. For example, questions about the exact phase coverage, whether the phases are commensurate or not, the Pb binding sites, the arrangement of the domain walls separating degenerate domains, the dependence of the phases on annealing, etc., remain. It is the purpose of this work to clarify most of these questions and to present a detailed atomic model of the structure of the dense α - $\sqrt{3}\times\sqrt{3}$ phase. This can stimulate theoretical work to calculate the strain driven interactions from first principles and to use them as input in statistical mechanics models to derive the observed phase diagram and to deduce the nature of phase transitions separating different phases.

The Pb phases observed at lower coverage (i.e., the mosaic phase at $\theta=1/6$ ML and the β - $\sqrt{3}\times\sqrt{3}$ at $\theta=1/3$ ML) are less controversial.³ We focus this work on the clarification of the structure of the dense, weakly bound α - $\sqrt{3}\times\sqrt{3}$ phase which forms around $\theta=4/3$ ML [unfortunately, this nomenclature is opposite to the one used for Pb/Ge(111)]. Because this phase is of higher density than the density of Pb(111) the Pb film are highly compressed. For example, the ideal commensurate phase $\sqrt{3}\times\sqrt{3}$ has 5% compression. Such compression is energetically costly and the system can gain energy by forming “light” domain walls (of lower density). Different phases are realized within a narrow coverage change since the domain-wall density can vary continuously with coverage and a variety of wall arrangements is possible.

In particular, two different phases have been discussed extensively: the HIC (i.e., hexagonal incommensurate phase)

and the SIC (i.e., striped incommensurate phase).⁴ The SIC has slightly higher Pb coverage and forms after annealing a small amount $\Delta\theta<0.02$ ML deposited on the HIC phase. Based on STM images, it was suggested that these phases are sixfold degenerate, which implies that Pb can occupy two different binding sites (i.e., H3 and T4) since the symmetry of the $\sqrt{3}\times\sqrt{3}$ unit cell is only threefold. A model for Pb/Ge(111) based on x-ray scattering has assigned H3 and off-centered T1 sites as the binding sites of the 4 Pb atoms in the ($\sqrt{3}\times\sqrt{3}$) unit cell.¹² However, no atomic model has been proposed of the exact atom arrangement, no determination of the binding sites has been made, and no correlation between electronic and real space structure has been suggested.

Information obtained with diffraction has been difficult to interpret since the superstructure spots related to the α - $\sqrt{3}\times\sqrt{3}$ phase do not appear at the expected commensurate wave vectors (1/3,1/3) and (2/3,2/3). This has led to the assignment of the phases as “incommensurate” although wave vectors different from the commensurate ones also result from regularity in the domain-wall distribution.^{4,5} At lower temperatures a different phase $\sqrt{7}\times\sqrt{3}$ is observed⁵⁻⁷ with incompatible coverage assignments for this phase $\theta=1$ ML⁶ vs $\theta=1.2$ ML.⁷ In addition, the nature of the high-temperature phase after heating to $T>270$ K, whether it is the HIC (Ref. 5) or the (1 \times 1) phase,⁶ is still not clear.

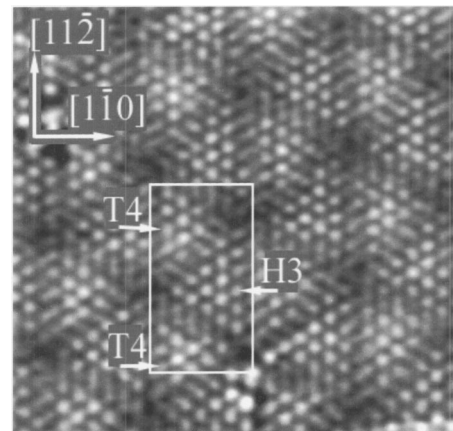


FIG. 1. 17.5 nm \times 15 nm STM image of the HIC phase showing the sixfold domain degeneracy, with alternating triangular domains occupying different binding sites H3 vs T4.

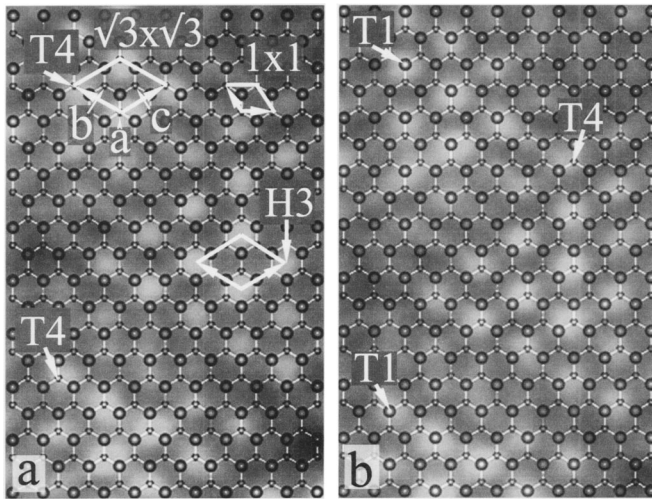


FIG. 2. A $\text{Si}(1 \times 1)$ lattice overlaid on top of the area in Fig. 1 enclosed by the white rectangle, can be used to deduce the type of site occupied in a given triangular domain, i.e., whether H3 or T4. Figure 2(a) is the correct assignment.

A high-resolution spot profile analysis–low-energy electron diffraction (SPA-LEED) study of the same system at $T > 300$ K has suggested that the HIC and SIC phases are commensurate phases with large unit cells $n \times \sqrt{3}$ ($n = \sqrt{3}1$ for the HIC and $n = 13$ for the SIC phase),⁸ but since the unit cell $\sqrt{3} \times \sqrt{3}$ was assigned coverage $\theta = 1$ ML as in an earlier STM study¹³ which has shown images with trimer structure, the domain walls are “heavy” and the coverage for the $n = 13$ phase is lower than the coverage of the $n = \sqrt{3}1$ phase. This is very puzzling because the SIC phase forms with the addition of Pb and, therefore, has higher coverage than the HIC phase.

It is clear that important information about the $\alpha\text{-}\sqrt{3} \times \sqrt{3}$ phase is missing or unclear. Since on this initial substrate phase intriguing self-organization phenomena have been observed with the further addition of Pb, as discussed elsewhere⁹ (i.e., for $\Delta\theta < 1$ ML regular two-dimensional cluster networks while for $\Delta\theta > 1$ ML uniform height islands form), it is important to clarify the open questions about the $\alpha\text{-}\sqrt{3} \times \sqrt{3}$ phase to attain a better understanding of the self-organization.

Figure 1 presents a high-resolution STM image of the HIC phase with six types of triangular domains arranged in hexagons. The white “blobs” within the domains correspond to the ideal $\sqrt{3} \times \sqrt{3}$ unit cell. The distance between two dark vertices of the triangular domains is 4.7 nm, which is close to $7\sqrt{3}a$, i.e., seven times the side of the $\sqrt{3} \times \sqrt{3}$ unit cell. Adjacent triangles have the high-symmetry Pb atoms in different binding sites (H3 or T4) marked in Fig. 2, which shows the area outlined by a white rectangle in Fig. 1. A comparison of the “blob” alignment along the $[11\bar{2}]$ direction shows a shift of 0.19 ± 0.03 nm (half the Si lattice constant 0.384 nm) in alternating triangles, which implies that alternating triangles occupy different sublattices (of the three possible sublattices, indicated by the letters a, b, c in Fig. 2, associated with a given binding site.)

In order to correlate the STM white “blobs” with the

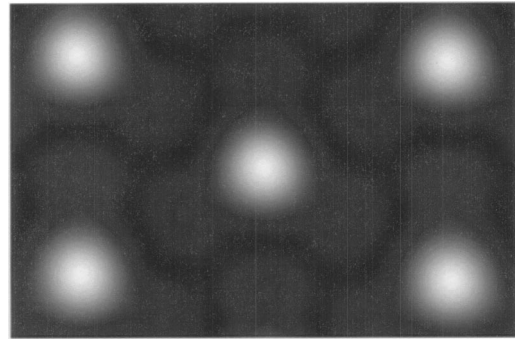


FIG. 3. First-principles calculation of the STM image of the $\alpha\text{-}\sqrt{3} \times \sqrt{3}$ for H3 site occupation with $V = +1.5$ V.

atomic positions in the $\sqrt{3} \times \sqrt{3}$ unit cell, we have performed first-principles density-functional calculations¹⁴ to study the structures, energies, and electronic properties of the dense $\alpha\text{-}\sqrt{3} \times \sqrt{3}$ phase. The calculations are performed using the pseudopotential and plane-wave basis set corresponding to a kinetic energy cutoff of 12 Ry. The local-density approximation is used with the Ceperley-Alder exchange-correlation functional¹⁵ parametrized by Perdew and Zunger.¹⁶ More details of the calculation will be published elsewhere.¹⁷ The calculation results show that the low-energy structures of the $\alpha\text{-}\sqrt{3} \times \sqrt{3}$ phase are the ones with three Pb atoms occupying T1 sites and a fourth Pb atom located at a high-symmetry site T4 or H3. These two sites have comparable binding energies with the energy of the T4 slightly lower by 4 meV/atom. Since the annealing temperature for the formation of the phases is approximately 500 K, the calculation results suggest that the two sites should have similar population in the HIC phase. As an illustration Fig. 3 shows the calculated STM image for H3 occupied site at a voltage of +1.5 V with the brighter spots corresponding to Pb atoms at the high-symmetry positions. The other three Pb atoms (at the T1 sites) which are bonded to the atoms at the H3 sites, have weaker intensity. The calculated result for T4 occupied sites is similar. We can therefore assign the white “blobs” in the experimental STM image to Pb atoms either in the H3 or T4 sites. In fact, at very small positive voltage $V = +0.1$ V, the experimental STM image reveals additional structures related to the three Pb atoms at the T1 sites and the Si atoms of the layer below, consistent with the theoretical results. This dependence of the imaged structures on tunneling voltage indicates that the difference between the intensity of the high symmetry and atoms at T1 sites is electronic and not geometric.

The separation between the “blobs” occupying adjacent domains can be used to identify the binding site (T4 or H3) within a given domain as shown in Fig. 2. An overlay of the underlying $\text{Si}(1 \times 1)$ lattice is superimposed on top of the image. If we assign the “blobs” of the middle domain to H3 sites in Fig. 2(a) and to T4 in Fig. 2(b) then the “blobs” in the adjacent domains are on T4 sites in Fig. 2(a) while in Fig. 2(b) they are on T1 sites. Since T1 are not the stable sites and no “blobs” are seen on these sites according to the theoretical calculation, it follows that Fig. 2(a) is the correct assignment.

Based on these observations we have built a unique model shown in Fig. 4 for the image of Fig. 1. The crystal $[11\bar{2}]$

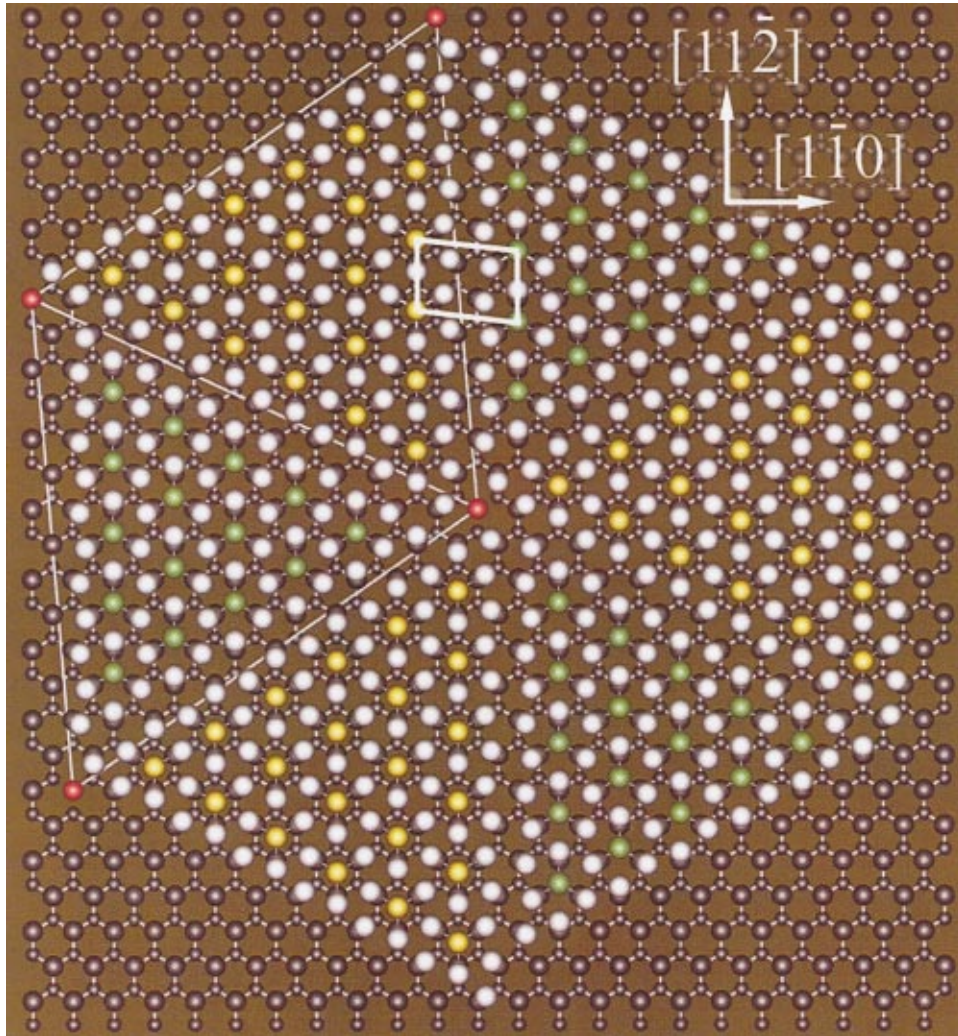


FIG. 4. (Color) Atomic model of the HIC phase shown in Fig. 1.

direction in Fig. 1 is essential for defining the model and is obtained experimentally from the direction of the faulted versus unfaulted (7×7) subcells on the clean surface. Each of the three $[11\bar{2}]$ row directions within a given triangle is aligned with a different direction of the three sublattices of the other binding site. Choosing one of the $[11\bar{2}]$ directions within a triangle (not parallel to the domain wall separating the chosen triangle from a neighboring triangle) the occupied sublattice within the neighboring triangle is fully determined from the width of the domain wall (i.e., the displacement vector of the domain wall has components $5/2a$ units parallel to and $a/\sqrt{3}$ normal to the $[1\bar{1}0]$ direction). Starting with a triangle of H3 sites colored “yellow” the type T4 sublattice occupied in the three neighboring triangles colored “green” is uniquely defined. The $[11\bar{2}]$ direction parallel to the domain wall separating the neighboring triangles determines the row within the “green” triangle to be used to select the H3 sublattice within the adjacent “yellow” site triangle. The same domain-wall width is used to determine which of the three “yellow” H3 sublattices is occupied next. Continuing the same procedure across the boundary between all adjacent triangles fully specifies the binding sites in all six domains around a common vertex. The selection of the domain-wall

width defines a $2.5 \times \sqrt{3}$ unit cell outlined in the figure.

The larger white-lined rhombus is the unit supercell of this structure. The side of this supercell is off the $[11\bar{2}]$ direction by an angle ϕ defined by $\tan \phi = 1/7\sqrt{3}$ (or $\phi = 5.2^\circ$). The “light” wall $2.5 \times \sqrt{3}$ “unit cell” is almost identical to the $\sqrt{7} \times \sqrt{3}$ (i.e., $2.64 \times \sqrt{3}$) unit cell (the small difference is related to the smaller shift $a/\sqrt{3}$ normal to the $[1\bar{1}0]$ direction from H3 to T4 sites versus $a\sqrt{3}/2$ shift for the $\sqrt{7} \times \sqrt{3}$ phase). The supercell can be thought as a combination of the ideal $\sqrt{3} \times \sqrt{3}$ in the domain interior and an almost $\sqrt{7} \times \sqrt{3}$ phase at the domain walls.

The diffraction pattern expected from the structure shown in Fig. 4, in general, will include additional closely spaced diffraction spots related to the larger size $7\sqrt{3}a$ of the supercell at positions other than the commensurate spot positions as observed with reflection high-energy electron diffraction and SPA-LEED. The location of the spots and their intensity level depends on the relative phase shift between the two adjacent triangles occupying different binding sites. We can estimate the domain-wall density as $0.28 wa^{-1}$ for the HIC phase of Fig. 4 as the ratio of the area covered by the domain wall $3 \times 7\sqrt{3}aw$ [w is the width of the domain wall and a the

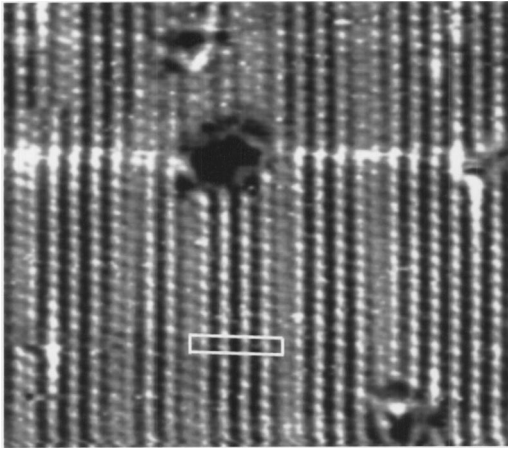


FIG. 5. 23 nm \times 20 nm STM image of the $n(\sqrt{7}\times\sqrt{3})+m(\sqrt{3}\times\sqrt{3})$ intermediate phase with $n=4$ and $m=1$, which forms with coverage between the ideal $(\sqrt{7}\times\sqrt{3})$ ($\theta=1.2$ ML) and HIC phase ($\theta=0.125$ ML).

Si(111) lattice constant] to the area of the supercell $(7\sqrt{3}a)^2(\sqrt{3}/2)$.

It is interesting to ask how the HIC structure (with $\theta=1.25$ ML in Fig. 4) develops out of the $\sqrt{7}\times\sqrt{3}$ phase ($\theta=1.2$ ML). Fig. 5 shows one of the structures formed prior to the formation of the HIC phase at slightly lower coverage. Such structure is an intermediate phase between the ideal $\sqrt{7}\times\sqrt{3}$ and the HIC phase built from a superposition of an integer number of $n\sqrt{7}\times\sqrt{3}$ and $m\sqrt{3}\times\sqrt{3}$ unit cells. The ideal $\sqrt{7}\times\sqrt{3}$ structure, with $\theta=1.2$ ML corresponds to $n=\infty$, $m=0$ while the ideal $\sqrt{3}\times\sqrt{3}$ with $\theta=4/3$ ML corresponds to $m=\infty$, $n=0$. The phase in Fig. 5 has $n=4$, $m=1$ with $\theta=1.217$ ML and unit cell $\sqrt{3}\times\sqrt{133}$ shown as a white parallelogram. Other intermediate phases with $1.2<\theta<1.33$ ML are built from specific pairs (n,m) as a result of long-range stress related interactions¹⁸ to be discussed elsewhere.¹⁹

If a small Pb amount $\Delta\theta>0.02$ ML is added on the HIC phase, the HIC phase converts to the SIC phase. The SIC

phase still has sixfold degenerate domains separated by the same $2.5a\times\sqrt{3}$ domain walls as in the HIC phase, but domain walls meander irregularly and their density is continuously lowered to accommodate the increasing coverage.

The domain-wall arrangement we propose and the intermediate (m, n) phases we discovered in the range $1.2<\theta<1.33$ ML can explain the conflicting literature results discussed earlier. For example, the $\sqrt{31}\times\sqrt{3}$ phase identified in Ref. 8 to be the HIC phase corresponds instead to an intermediate phase with $n=1$, $m=2$ [i.e., 1 unit cell of the $\sqrt{7}\times\sqrt{3}$ and 2 unit cells of the $\sqrt{3}\times\sqrt{3}$ phase with the superstructure unit cell side $\{((5/2)+2(3/2))^2+(\sqrt{3}/2)^2\}^{0.5}=\sqrt{31}$] while the $13\times\sqrt{3}$ phase identified as the SIC phase possibly corresponds to the $n=1$ and $m=7$ phase. As will be discussed in Ref. 19, if $m+n$ is odd the side of the superstructure unit cell is an irrational number while if it is even the side is an integer number. This assignment explains why the coverage of the $\sqrt{31}\times\sqrt{3}$ phase is lower than the coverage of the $13\times\sqrt{3}$ phase (while in the proposed model of Ref. 8 the coverage is higher). In addition, our results settle the disagreement about the $\sqrt{7}\times\sqrt{3}$ coverage since they suggest that $\theta=1.2$ ML as in Ref. 7.

In summary, based on STM measurements and first-principles calculations we have determined the atomic model and domain-wall arrangement of the dense Pb/Si(111)- $\alpha\sqrt{3}\times\sqrt{3}$ phase. Two different sites H3 and T4 of comparable binding energies are occupied and result in the formation of sixfold degenerate domains for the HIC and SIC phases. Prior to the formation of these phases, other intermediate phases form by combining integer number of $\sqrt{7}\times\sqrt{3}$ and $\sqrt{3}\times\sqrt{3}$ unit cells which can explain the complex (and seemingly conflicting) diffraction patterns observed within a small coverage variation.

Ames Laboratory is operated by the U.S. Department of Energy by Iowa State University under Contract No. W-7405-Eng-82. This work was supported by the Director for Energy Research Office of Basic Energy Sciences.

¹P. J. Estrup and J. Morrison, Surf. Sci. **2**, 465 (1964).

²G. Le Lay *et al.*, Surf. Sci. **204**, 57 (1988).

³E. Ganz *et al.*, Surf. Sci. **257**, 259 (1991).

⁴L. Seehofer *et al.*, Phys. Rev. B **51**, 13 503 (1995).

⁵K. Horikoshi *et al.*, Phys. Rev. B **60**, 13 287 (1999).

⁶J. Slezak *et al.*, Phys. Rev. B **60**, 13 328 (1999).

⁷Ch. Kumpf *et al.*, Surf. Sci. **448**, L213 (2000).

⁸A. Petkova *et al.*, Surf. Sci. **471**, 11 (2001).

⁹M. Hupalo and M. C. Tringides, Phys. Rev. B **65**, 205406 (2002).

¹⁰J. V. Barth *et al.*, Phys. Rev. B **42**, 9307 (1990).

¹¹O. L. Alerhand *et al.*, Phys. Rev. Lett. **61**, 1973 (1988).

¹²S. A. de Vries *et al.*, Phys. Rev. B **59**, 13 301 (1991).

¹³I. S. Hwang *et al.*, Phys. Rev. B **51**, 10 193 (1995).

¹⁴P. Hohenberg and W. Kohn, Phys. Rev. **136**, B864 (1964); W. Kohn and L. J. Sham, Phys. Rev. **140**, A1135 (1965).

¹⁵D. M. Ceperley and B. J. Alder, Phys. Rev. Lett. **45**, 566 (1980).

¹⁶J. P. Perdew and A. Zunger, Phys. Rev. B **23**, 5048 (1981).

¹⁷T. L. Chan *et al.* (unpublished).

¹⁸P. Bak, Rep. Prog. Phys. **45**, 587 (1982).

¹⁹M. Hupalo and M. C. Tringides (unpublished).